CPC(HEP & NP), 2012, **36**(4): 376–379 **Chinese Physics C** Vol. 36, No. 4, Apr., 2012

Design and simulation of a C-band pulse compressor

XIAO Ou-Zheng(肖欧正) ZHAO Feng-Li(赵风利) HE Xiang(贺祥)

Institute of High Energy Physics, Chinese Academy of Sciences, Beijing 100049, China

Abstract: The design and optimization procedure of a pulse compressor is presented. A C-band (5712 MHz) pulse compressor using a $TE_{0,1,15}$ mode cylindrical cavity with dual side-wall coupling irises has been designed. Also the coupling coefficient, position of the short plane and size of the bottom groove have been optimized by using HFSS.

Key words: pulse compressor, energy multiplication factor, coupling coefficient

PACS: 29.20.-c **DOI:** 10.1088/1674-1137/36/4/015

1 Introduction

During the development of pulse compressors, much progress has been made in improving the efficiency and enhancing the power gain. Besides the SLAC Energy Doubler (SLED), several other compression schemes producing a flat output pulse have been explored, such as the SLED II, the Binary Pulse Compressor (BPC) and so on. Compared with the S-band accelerator, there are many advantages to the C-band accelerator, such as its compact structure, high accelerating gradient and high efficiency, which has driven research in C-band pulse compressors. A scaled down model of the S-band used in the BEPC II linac has been considered, but a sufficient Q factor cannot be acquired. Another design plan is needed. We considered adopting a cavity using a $TE_{0,1,15}$ mode in the coupled cavity pulse compressor [1]. The Q factor is about 180000 and the maximum energy multiplication factor can reach 1.91 analytically.

2 Design and optimization procedure

The pulse compressor is composed of two identical high-Q factor cavities attached to a 3-db coupler. The performance of the pulse compressor depends on the design of storage cavities. The energy multiplication factor M can be expressed as [2]:

$$M=\gamma \mathrm{e}^{-T_\mathrm{a}/T_\mathrm{c}}\left[1-(1-g)^{1+v}\right]\left[g(1+v)\right]^{-1}-\alpha+1, \qquad (1)$$

where T_a is the filling time of the accelerating structure, T_c is the filling time of the cavity, $\alpha=2\beta/(1+\beta)$, $\nu=T_\mathrm{a}/T_\mathrm{c}[\ln(1-g)]^{-1}$, g is the gradient of group velocity along accelerating structure, $\gamma=\alpha(2-\mathrm{e}^{-t/T_\mathrm{c}})$, β is the cavity coupling coefficient. When the coupling factor is optimized to give the maximum energy gain, it shows that the longer the pulse length and the higher the unloaded Q, the greater the energy gain.

We summarize the design and optimization procedure of the pulse compressor as follows.

(1) Choose the storage cavity mode

A cylindrical cavity with $TE_{0,n,p}$ mode possesses a high Q factor and has no degenerate mode except for $TM_{1,n,p}$, so $TE_{0,n,p}$ as the cavity mode is a good choice. The Q factor can be expressed as [3]:

$$Q_0=\frac{\lambda*[\upsilon_{mn}^2+(p\pi R/l)^2]^{\frac{3}{2}}}{2\pi\delta\left[2p^2\pi^2\dfrac{R^3}{l^3}+\upsilon_{mn}^2\right]}. \qquad (2)$$

We can determine the cavity mode based on the Q factor that should meet the engineering requirement of the energy multiplication factor.

(2) Optimize the cavity diameter to obtain the maximum frequency separation [4]

The relation among resonant frequency, mode and geometry dimensions can be expressed as:

$$\left(\frac{f_0D}{c}\right)^2=\left(\frac{\upsilon_{mn}}{\pi}\right)^2+\left(\frac{pD}{2l}\right)^2 (p\neq 0). \qquad (3)$$

The axial and radial dimensions of the cavity vary at the same time to keep the frequency of the $TE_{0,1,15}$ mode constant, whereas all other resonant frequencies vary and produce traces across the mode chart. Fig. 1 and Fig. 2 show the mode charts with $TE_{0,1,15}$ at 5712 MHz.

Received 19 July 2011

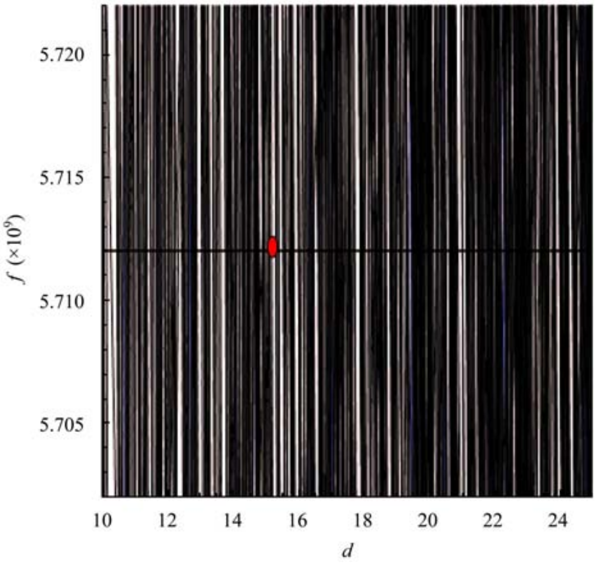

Fig. 1. $TE_{0,1,15}$ at 5712 MHz mode chart with the design value marked with a red circle.

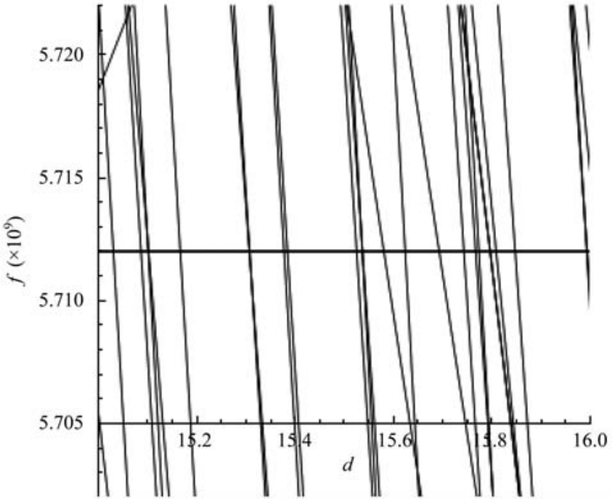

Fig. 2. Close-up mode chart diameter from 15 cm to 16 cm.

Considering the cost, unloaded Q factor, mechanical stability and frequency separation of competing modes, it is preferable to choose a cavity diameter of 15.26 cm, and then the cavity height should be 43.358 cm.

(3) Optimize the coupling factor to get the maximum energy multiplication factor

The main characteristics of the accelerator RF parameters are shown in Table 1. Using these values, we can get Fig. 3, which shows the relation between coupling factor β and the energy multiplication factor.

Figure 3 shows that the energy multiplication factor obtains the maximum value of 1.91 while the coupling coefficient is 8.03.

Table 1. RF parameters.

frequency	5712 MHZ
Q	180000
T_a	0.4 μs
g	0.6
pulse width	2.5 μs
pulse width before phase inversion	2.1 μs

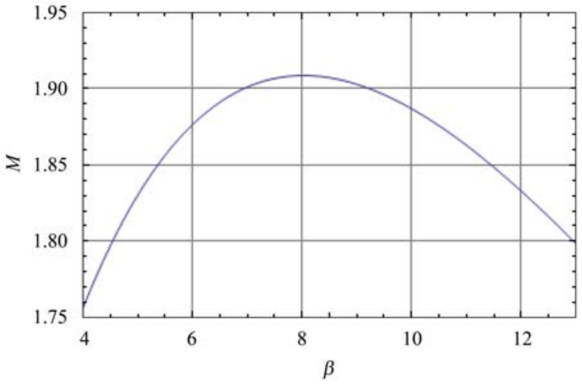

Fig. 3. Energy multiplication factor as a function of coupling factor β.

3 Coupling method

There are two coupling methods in the SLED system, dual-iris and single-iris. We prefer the former considering the power capacity. The cavity is coupled to the waveguide through two holes, which are half a wavelength away from each other on the sidewall of the waveguide. According to Bethe theory, the apertures can be equivalent to a pair of opposite magnetic dipoles. The dot product between the dipoles and magnetic field of $TE_{0,1,15}$ are mutually reinforced, and cancel out each other in the case of $TM_{1,1,15}$. There is only a longitudinal magnetic field component like Sinusoidal variation along the sidewall of rectangular waveguide. The position of the short plane is optimized to about $(2n+1)/4$ waveguide wavelength in order to maximize β. Compared with single-iris, there are many advantages of dual-iris [5]:

(1) improving the power capacity and avoiding sparking;

(2) suppressing the degenerate mode $TM_{1,1,15}$; and

(3) coupling coefficient adjustment is more convenient by changing the position of the short plane.

The coupling coefficient is determined by the aperture size, magnetic strength at the apertures and the location of the short plane. Coupling factor as a function of iris radius and height can be expressed as [6]:

$$\beta = kR^6 e^{-2\alpha d}, \tag{4}$$

where k is a constant to be determined, R is the radius of aperture, d is the height of aperture, α is the attenuation coefficient. Practically, if one value of β is known by means of experiments or theoretical calculations with respect to one size of a coupling aperture, the other values of β corresponding to other different sizes of coupling apertures can be scaled.

4 Optimization of the bottom groove

There are some parasitic modes and a degenerate mode $TM_{1,1,15}$ near $TE_{0,1,15}$, which will seriously affect the performance of the cavity, so they must be suppressed. The parasitic modes can be suppressed by optimizing the cavity dimensions, but this does not work for the degenerate mode. According to the characteristics of electromagnetic field distribution and Slater's perturbation theory, we can cut a circular groove in one end-plate. This groove does not disturb the $TE_{0,1,15}$ mode field pattern or frequency. Table 2 summarizes the results of our analytical calculations and simulation of various modes around 5712 MHz (C-band) for a cavity with diameter 152.6 mm and length 433.58 mm. Table 3 shows the results of simulation of various modes around 5712 MHz after the groove is optimized with a width of 4.5 mm and depth of 4.6 mm.

Table 2. Modes around $TE_{0,1,15}$.

modes	analytical calculations/MHz	simulation by HFSS/MHz	frequency separation/MHz
$TM_{4,1,9}$	5674.42	5675.87	−38.16
$TM_{0,3,5}$	5680.9	5682.59	−29.99
$TE_{0,1,15}$	5712.58	5713.42	0
$TM_{1,1,15}$	5712.58	5713.42	0
$TE_{3,2,8}$	5724.68	5726.33	+12.91
$TE_{1,3,6}$	5726.96	5728.74	+14.48
$TM_{0,1,16}$	5732.26	5733.44	+19.68
$TE_{5,1,5}$	5751.09	5752.71	+38.51

Table 3. Modes around $TE_{0,1,15}$ after the groove is optimized.

modes	simulation by HFSS/MHz	frequency separation/MHz
$TE_{0,1,15}$	5713.41	0
$TM_{1,1,15}$	5702.35	−11.06
$TM_{0,1,16}$	5724.32	+10.91
$TM_{3,1,12}$	5725.72	+12.31

5 Results of simulation by HFSS

After the previous theoretical analysis, we have carried out three-dimensional field calculations by HFSS to find the optimal size of the coupling apertures and the position of the short plane. Fig. 4, Fig. 5 and Fig. 6 show the relation between β and the radius of the coupling aperture, the relation between β and height of the coupling holes, the relation between β and position of the short plane respectively. Fig. 7 and Fig. 8 show the electric and magnetic fields for a dual-iris SLED system.

The diameter and height of the coupling aperture were chosen to be 18.68 mm and 4 mm, respectively. The position of a short plane is optimized in order to maximize β. It is about 3/4 wave length which corresponds to the plunger position 49.75 mm away from one of the coupling holes. Then the coupling coefficient is 8.11. We usually chamfer the coupling holes in order to reduce the maximum electric field strength at the coupling apertures to prevent breakdown, which will result in a coupling coefficient increase. However, we can adjust the position of the short plane to make the coupling coefficient in the best condition.

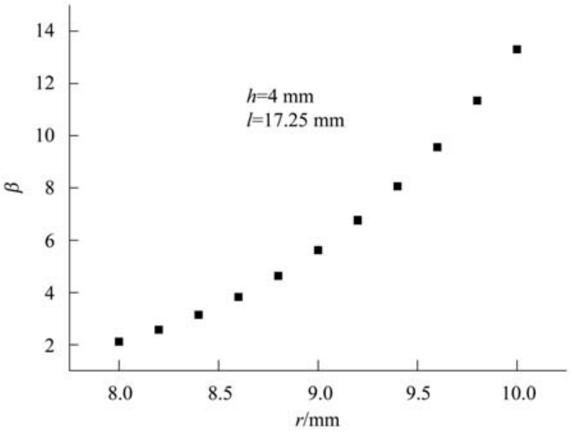

Fig. 4. Coupling coefficient as a function of aperture radius.

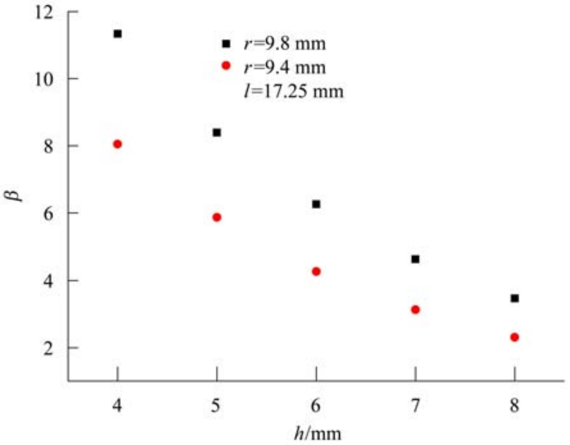

Fig. 5. Coupling coefficient as a function of aperture height.

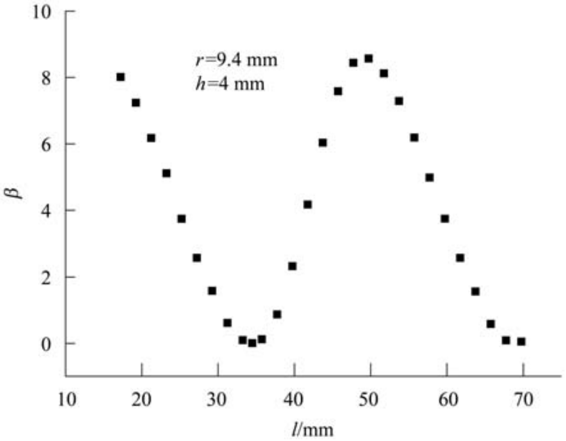

Fig. 6. Coupling coefficient as a function of short plane position.

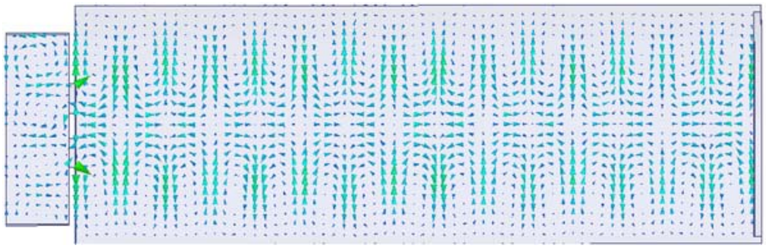

Fig. 7. Magnetic field in the SLED cavity calculated by HFSS.

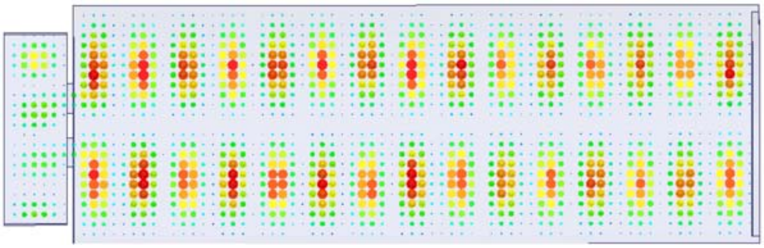

Fig. 8. Electric field in the SLED cavity calculated by HFSS.

6 Conclusion

Pulse compressors, as a key technology for particle accelerators, have been widely studied at national accelerator laboratories, such as KEK, CERN and SLAC, but there are only a few studies on the C-band. We designed a C-band SLED using a $\mathrm{TE}_{0,1,15}$ mode cylindrical cavity with dual side-wall coupling irises. The theoretic calculation and the simulation results match well, and a C-band SLED will be fabricated in the future.

I would like to express my sincere thanks to Professor Hou Mi and Dr. Zhai Ji-Yuan for their kind help.

References

1 Shintake T, Akasaka N, Matsumoto H. Development of C-band RF Pulse Compression System for e^+e^- Linear Collider. Proc. of the 17th IEEE Conf. on Particle Accelerator. Vancouver, 1997. 455–457

2 Farkas Z D, Hogg H A, Loew G A et al. A Method of Doubling SLAC' Energy. SLAC-PUB-1453, 1974

3 YAN Yun-Qing, LI Ying-Hui. Foundation of Microwave Technology. Second Edition. Beijing: Beijing Institute of Technology Press, 1997. 230–240

4 Fiebig A, Hohbach R, Marchand P et al. CERN/PS 87-45(RF), 1987

5 Matsumoto H, Baba H, Yamaguchi S. Nucl. Instrum. Methods Phys. Res. A, 1993, **330**: 1–11

6 GAO J. Nucl. Instrum. Methods Phys. Res. A, 2002, **481**: 36–42